Fast laser micromachining of micro-optics in quartz and BaF_2

G. Kopitkovas*, T. Lippert*, C. David*, A. Wokaun* and J. Gobrecht*

*Paul Scherrer Institut, CH-5232, Villigen-PSI, Switzerland
E-mail: thomas.lippert@psi.ch

Micro-lenses in quartz and BaF_2 are fabricated using a one step technique which utilizes Laser Induced Backside Wet Etching and the projection of a Diffractive Gray Tone Phase Mask. The structuring of quartz and BaF_2 is achieved using 308 nm irradiation and laser fluences well below the ablation threshold of these materials. The key element in this process is an organic liquid which is in contact with the quartz or BaF_2 substrate. The strong absorption of the laser light in a thin liquid layer at the substrate interface results in the creation of high temperature and pressure jumps, which are the key elements in the etching process.

DOI: 10.2961/jlmn.2006.01.0005
Keywords: quartz, BaF_2, wet etching, micro-optics, beam homogenizer

1. Introduction

UV transparent dielectric materials, e.g. quartz and BaF_2 are very important materials in optics. Arrays of micro-optical elements fabricated in quartz or in BaF_2 are used as beam homogenizers for high power lasers. Homogenization of the laser beam intensity is usually achieved by the combination of a plano convex micro-lens array and a plano convex lens. The micro-lens array splits the incoming laser beam intensity into a number of beamlets, which overlaps at the focal plane of the collecting lens, resulting in the creation of a homogeneous laser beam profile [1].

Fabrication of micro-optical components with continuous profiles in quartz or BaF_2 is a complicated process, mainly due to the strong mechanical properties of these materials. The conventional technique which is used for structuring of micro-optical components in quartz and in BaF_2 is the combination of photolithography, resist melt techniques and Reactive Ion Etching [2]. This method usually requires high vacuum conditions and a high control of the proportional etching process during ion etching. Other methods for the structuring of quartz are the direct laser ablation using ultrafast or Vacuum Ultraviolet (VUV) lasers. The roughness of the etched features in quartz by the ultrafast lasers, however, is in the micrometer range, which is too high for optical applications [3, 4]. The etch roughness of quartz substrates structured with direct ablation by F_2 excimer laser (157 nm, 11 ns) are in the range of 40 nm [5]. This technique can be applied for direct micromachining of quartz, however, it requires expensive optics and transparent gases for the beam path.

An alternative method for the structuring of the UV transparent materials, e.g. quartz or CaF_2 has been developed by Niino et al [6-9]. This method is known as a Laser Induced Backside Wet Etching (LIBWE). KrF or XeCl excimer lasers can be applied as irradiation sources in this approach. Quartz or BaF_2 substrates are transparent for the applied wavelengths and can only be directly ablated at very high laser fluences (>20 J/cm^2). In order to achieve absorption of the laser photons a strong absorbing organic liquid is applied, which is in contact with the UV transparent material. During the irradiation a high temperature jump is created at the thin interface between the substrate and liquid, which results in several effects, e.g. softening or melting of the UV transparent material, and the creation of a high pressure jump, which is a result of the boiling of the solution [6-14]. These effects are the key elements in LIBWE process.

Precise structuring of quartz by LIBWE, with etch rates of more than 100 nm per pulse and etch roughness of less than 10 nm have been demonstrated [6-9, 13, 17]. Submicron spaced gratings in quartz could be fabricated by utilizing an interference setup and LIBWE [15]. The combination of LIBWE and projection of a Diffractive Gray Tone Phase Mask (DGTPM) can be applied as an alternative technique for the fabrication of micro-optical components in quartz [13, 14, 16]. The key element in this approach is the DGTPM which is used to modulate the incoming beam intensity. The modulated beam is projected onto the backside of the UV transparent materials, where etching occurs. Recently we have been optimizing the etching parameters in order to fabricate high quality micro-lenses in quartz. The plano-convex micro-lenses have been tested as beam homogenizers for a quadrupled Nd:YAG laser.

2. Experimental

A quartz plate with a thickness of 0.5 mm was applied as sample, while the thickness of the BaF_2 substrates was 2 mm. The plano-convex micro-lens arrays were fabricated in quartz substrates with a thickness of 2.3 mm. The surface roughness was 4 nm for all samples. A XeCl excimer laser (308 nm, 20 ns) is used as irradiation source with a repetition rate of 5 Hz. 0.4 M pyrene in acetone and 1.4 M pyrene in tetrahydrofuran (THF) solutions were applied as etching media.

A refractive doublet lens system (10x demagnification) was applied for imaging of the DGTPM (as shown in Fig 1).

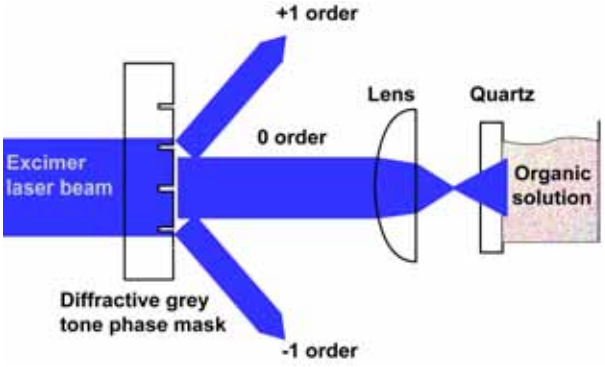

Fig. 1 Experimental setup for the fabrication of micro-optics in quartz.

The depth profile of the etched features in quartz and in BaF_2 was examined with a profilometer (DEKTAK 8000).

3. Results and Discussion

A possible mechanism for the LIBWE process is based on the strong absorption of the intense laser light by the organic liquid, which is in contact with the UV transparent material. Rapid relaxation processes of the excited dye molecules generate a fast increase of the temperature at the substrate-liquid interface and may result in softening, melting or even boiling of the surface of the UV transparent materials. Secondary processes which take place at the thin layer between the substrate and the liquid are the creation of the shock wave and the boiling of the solvent. The latter results in the creation of expanding and collapsing bubbles, which generate a strong pressure jump at the interface between the heated material and the liquid. The pressure jump from the shock wave or from the bubble may remove the softened material from the surface.

One characteristic of the structuring of UV transparent materials by LIBWE is the existence of a threshold fluence. The threshold fluence for quartz is defined as the lowest fluence, for which no etching can be achieved. In the case of BaF_2 the threshold fluence is defined as the lowest laser fluence, for which the etching can be quantified. Etching of BaF_2 is achieved at fluences below the defined threshold value, but it is impossible to determine a etch depth due to very low etch rates and very high etch roughness. The experimentally obtained threshold fluences for SiO_2 and BaF_2 using two different solutions are summarized in Table 1 together with some thermodynamic properties of these materials.

Table 1 The etching thresholds of quartz and BaF_2 and some thermodynamic and mechanical properties

	SiO_2	BaF_2
Threshold fluence, J/cm^2 c=0.4 M (Pyrene/Acetone)	0.66	0.81
Threshold fluence, J/cm^2 c=1.4 M (Pyrene/THF)	0.48	0.57
Melting temperature, °C	1600	1280
Thermal diffusivity, m^2/s	$8.4 \cdot 10^{-7}$	$5.8 \cdot 10^{-6}$
Rupture modulus, MPa	50	26

The reason why the threshold fluence obtained for quartz is lower than the threshold fluence for BaF_2 is most probably associated with the mechanical properties of these materials, but my also be influenced by the very different etch roughness for these materials.

The etch rates obtained for quartz and BaF_2 are obtained experimentally by measuring the depth of the etched features at various laser fluences as function of the number of laser pulses. Similar etch rates (shown in Fig. 2) are observed for both materials at laser fluences below 1.7 J/cm^2 using the 0.4 M pyrene in acetone solution.

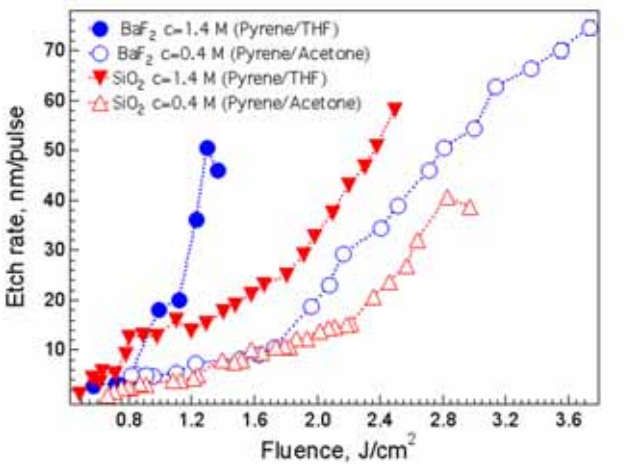

Fig. 2 The etch rates of quartz and BaF_2 using different etching media.

The similar etch rates of quartz and BaF_2 in the fluence range of 0.8 J/cm^2 to 1.7 J/cm^2 are difficult to explain only by mechanical or thermodynamical properties of the material. The similar etch rates could be related to the material properties but may also be influenced by a possibility of different etching processes which occurs for quartz and BaF_2. Detailed studies on the etching process are in progress.

The increase of the etch rates at laser fluences above 1.7 J/cm^2 for BaF_2 and at laser fluence above 2.2 J/cm^2 for SiO_2 for the 0.4 M solution is probably associated with a change in the etching mechanism, which will be discussed in detail later. The increase of the etch rates and decrease of the threshold fluences was achieved for both materials by increasing the pyrene concentration in the solution. The higher pyrene concentration causes the generation of a higher temperature jump at a thinner substrate-liquid interface.

The etching of UV transparent materials by LIBWE is a complex process, where several etching mechanisms are present [10, 13, 17]. The etching of quartz does not start with the first laser pulse when the laser fluence is below 0.8 J/cm^2 using the 1.4 M pyrene in THF solution as etching media (shown in Fig. 3). A very similar behavior is also obtained for the BaF_2 samples, which is also shown in Fig. 3. Incubation effect is also observed using 0.4 M pyrene in acetone solution as etching media [13, 18].

The low etch rates and strong incubation effect observed for quartz and BaF_2 at the low laser fluences is probably due to a lower temperature jump which is not sufficient to achieve softening or melting of the material. The temperature jump is, however high enough to decompose the solution, resulting in the generation of carbon deposits [13, 18]. The carbon strongly adheres to the surface of the substrate and increases therefore the absorption of the laser energy. This results in a higher temperature jump, which may cause the softening-melting of the materials. The removal of the material at low laser fluences is clearly influenced by the formation of a carbon layer.

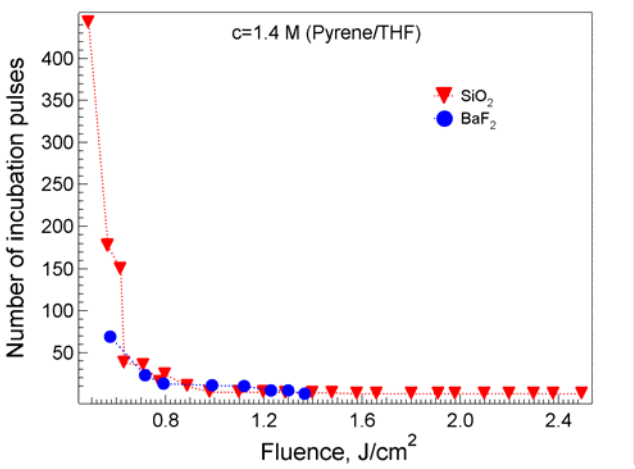

Fig. 3 Number of incubation pulses required for initiating the etching process in quartz and BaF_2.

The increase of the etch rates by increasing laser fluences (above 1.2 J/cm^2 in the case of 0.4 M pyrene in acetone solution and above 0.8 J/cm^2 in the case of 1.4 M pyrene in THF solution) is associated with the generation of higher temperature jumps. An increase of the temperature causes also stronger pressure jumps, which remove the softened – molten material within several laser pulses.

The etch rate slope is changing again at high laser fluences (>2.2 J/cm^2 for the quartz at the low concentrated solution and >1.8 J/cm^2 using a high concentrated solution). In this fluence ranges very high temperature jumps are obtained which result in the generation of a plasma in the solution. The plasma assists probably the etching process yielding the high etch rates. An increase of the etch rates at high laser fluences is also observed for the BaF_2 samples, but at lower laser fluences compared to quartz. The reason why a lower "plasma threshold" fluence is obtained for BaF_2 may be related to the mechanical and thermal properties of this material. For laser fluences above 1.3 J/cm^2 (for 1.4 M pyrene in THF solution) cracks are observed in the BaF_2 surface. This is probably due to the stronger pressure jump, which may exceed the rupture modulus of the hot material.

The roughness of the etched features in quartz is strongly influenced by the applied laser fluences (shown in Fig. 4) and can also be divided into several regions. High etch roughness in quartz are observed at the low laser fluences (just above the threshold fluence), which is probably associated with the formation of the amorphous carbon layer on the surface of the substrate. The roughness of the etched areas in quartz is then strongly decreasing with increasing laser fluence. The lowest etch roughness (≈20 nm) for structuring of quartz is observed within the laser fluence range which is marked in the Fig. 4. This fluence range is applied for the fabrication of micro-optical components in quartz.

The increase of the etch roughness in quartz with the higher laser fluences (above the fluence of 2.2 J/cm^2) is most probably due to interaction of the plasma with the quartz surface.

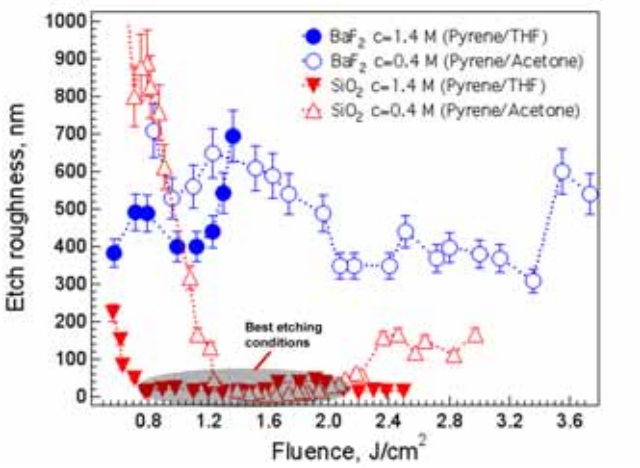

Fig. 4 The roughness of the etched features in quartz and in BaF_2 using different etching solvents.

The roughness of etched features in BaF_2 does almost not depend on the laser fluence and is always in the range from 360 to 700 nm. The lowest roughness of the etched features (≈360 nm) obtained for BaF_2 is at least 20 times higher than the lowest roughness observed for quartz (≈15 nm). This is most probably associated with the lower mechanical stability and resistance to the temperature and pressure jumps of BaF_2. The mechanical stability of a material is expressed by the modulus of rupture, which is defined as the load which is required to break a bar of one inch square. The values of the modulus of rupture for the different UV transparent materials are included in Table 1. An increase of the applied pressure above the modulus of rupture results in the generation of cracks and damaging of the material. The values of this critical load pressure obtained for quartz is much higher than the values for BaF_2. The lower mechanical stability of BaF_2 may be the origin of the higher etch roughness as compared to quartz. The quality of the etched areas in BaF_2 does also not improve with an increase of the pyrene concentration in solution, while in the case of quartz higher concentrated solutions lead to a decrease of the etch roughness (shown in Fig 4). The reason for the improvement of the etching quality in quartz, with increasing of the pyrene concentration in the solution is related to the increase of the temperature and pressure jumps in the thinner liquid layer at the substrate interface. An increase of the temperature causes melting of the quartz surface which will be reached at lower laser fluences using 1.4 M pyrene in THF solution as etching media. However, an increase of the pyrene concentration in the solution does not improve the quality of the etched features in BaF_2

substrates (shown in Fig. 4). The roughness remains almost the same for the higher pyrene concentration in the solution. This is probably due to the material properties of BaF_2 or a higher sensitivity to pressure and temperature jumps.

The optimum etching conditions have been applied to fabricate micro-optical components. One of the most important commercial application of micro-optical components fabricated in quartz is laser beam shaping and homogenizing. The homogenizing of high power lasers requires an array of plano-convex micro-lenses fabricated in a UV transparent material, e.g. quartz. The micro-lens array splits the incoming laser beam intensity into a number of beamlets, which are collected in the focal plane of the collecting lens, as shown in Fig. 5.

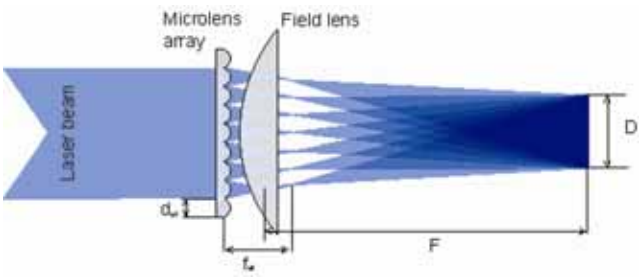

Fig. 5 Experimental setup for beam homogenizing

The homogenized beam size D obtained at the focal plane of the collecting lens is proportional to focal length of the collecting lens, diameter and the focal length of the micro-lens, and can be calculated using equation (1):

$$D = \frac{d_{\mu l} \cdot F}{f_{\mu l}} \qquad (1),$$

where d_{ul} and f_{ul} are the diameter and the focal length of the micro-lenses and F is the focal length of the collecting lens.

An array of plano-convex micro-lens was fabricated in quartz by the combination of LIBWE and projection of a Diffractive Gray Tone Phase Mask. A 3 D image of a hexagonaly closely packed plano convex micro-lens array in quartz is shown in Fig. 6.

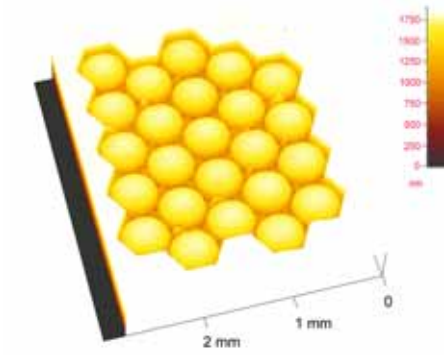

Fig. 6 3 D image of the plano-convex micro-lens array fabricated in quartz.

The diameter of each micro-lens is 500 um, while the focal length of the micro-lenses is 70 mm. The focal length of the micro-lenses is obtained from the line scan profile, which is shown in Fig. 7.

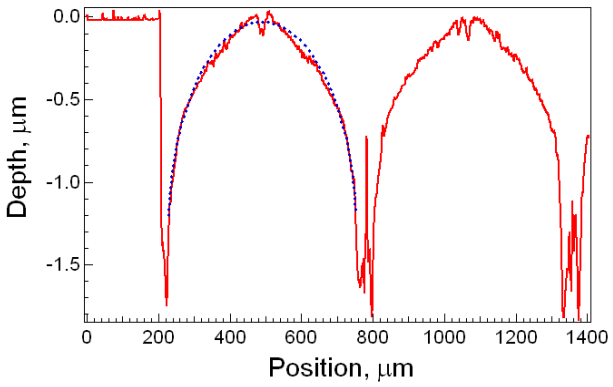

Fig. 7 The depth profile of the micro-lens array fabricated in quartz.

The micro-lens has a parabolic shape, which is fitted with a parabolic function (dotted line in Fig. 7), that has been described previously [13]. The good agreement between the measured parabolic profile of the micro-lens and theoretical fit suggests the ability to use this technique for the fast fabrication of micro-lenses in UV transparent materials.

The homogenizing of a Nd:YAG laser beam profile was tested with a quartz micro-lens array which consists of 20x22 micro-lenses. The etching conditions were the same as for the test micro-lens array shown in Fig. 6. The focal length of the collecting lens used for the homogenizing of the Nd:YAG laser was 250 mm. The Nd:YAG laser beam profile with and without the beam homogenizer is shown in Fig. 8. The homogenized beam size obtained at the focal plane of the collecting lens is 1.6 mm, which corresponds well to the value calculated from equation (1).

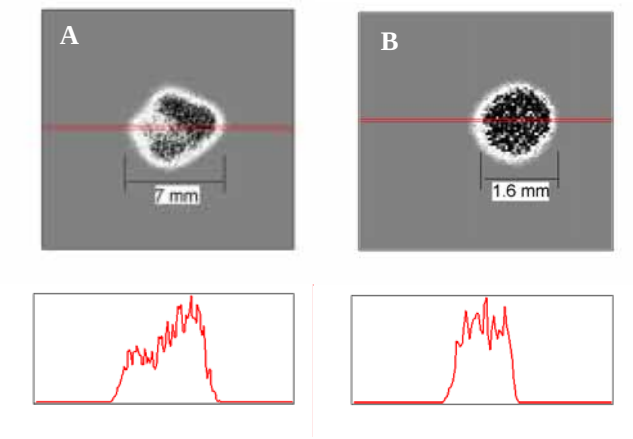

Fig. 8 The spatial beam profile of a quadrupled Nd:YAG laser without (A) and with beam homogenizer (B).

A clear improvement of the Nd:YAG laser beam profile is obtained when the micro-lens array is applied. However, the line scan profile suggests the existence of energy fluctuations in the intensity of the homogenized laser beam, which are in the range of 30 % (RMS). These energy

fluctuations are most probably caused by an interference effect, resulting from dividing of the laser beam into a number of beamlets. This interference effect is associated with the coherence of the laser and depends on the diameter of the micro-lens and the focal length of the collecting lens. An improvement of the micro-lenses is necessary to achieve a more homogenous laser beam profile.

The combination of LIBWE and projection of a DGTPM can be applied, as discussed above, for the fabrication of more complex structures than plano-convex micro-lenses in UV transparent materials. The fabrication of complex structures, e.g. Fresnel micro-lenses in quartz and in CaF_2 have been reported previously [14, 16] and was now also achieved for BaF_2 (shown in Fig. 9).

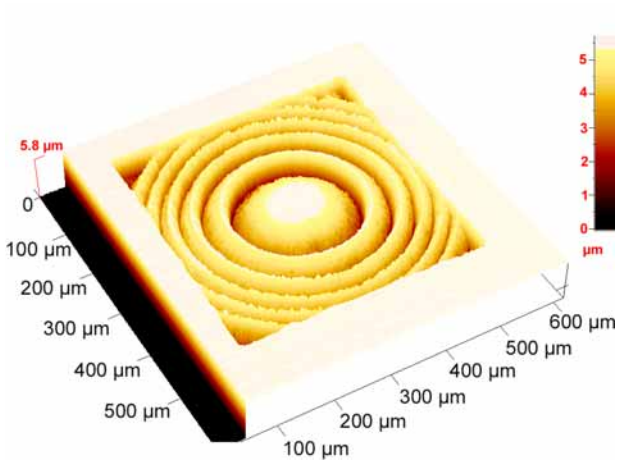

Fig. 9 3 D image of the Fresnel micro-lens in BaF_2.

The line scan of the Fresnel lens fabricated in BaF_2 (shown in Fig 10) presents the typical features of a Fresnel lens: a parabolic depth profile in the center and triangular structures on the sides.

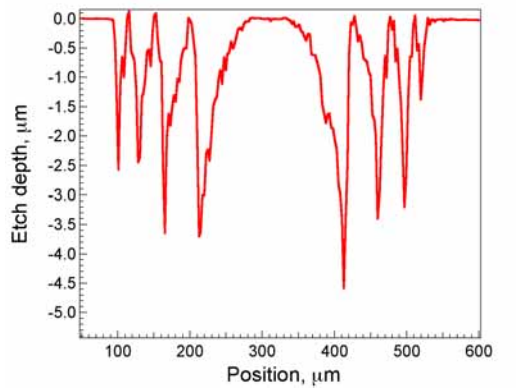

Fig. 10 Depth profile of the Fresnel lens fabricated in BaF_2.

This micro-lens could not be applied for the UV applications due to the relatively high etch roughness (300 nm), but it can be used as a diffractive optical component in the near and Infrared wavelength range.

4. Conclusions and outlook

The combination of LIBWE with the projection of a Diffractive Gray Tone Phase Mask is an alternative technique for the one step fabrication of micro-optical components in UV transparent materials. This technique requires a conventional XeCl excimer laser and a Diffractive Gray Tone Phase Mask. The laser fluences are well below the ablation-damage fluence of these materials.

A clear improvement of the Nd:YAG laser beam homogenizing is obtained for applying a micro-lens arrays which has been fabricated in quartz by LIBWE.

Etching of UV transparent materials by LIBWE is a complex process, where etch rates and etch roughness are strongly influenced by the high pressure and temperature jumps. This interplay between the temperature and pressure increase results in several mechanisms of removal of the heated/softened or molten material from the surface. The key question of LIBWE mechanism is when the removal of the UV transparent material takes place.

References

[1] O. Homburg, B. Finke, P. Harten, L. Lissotsenko: EuroPhotonics, **7,** (2003) 34.
[2] S. Sinzinger, J. Jahns: "Microoptics" 2nd ed., (Wiley-VHC GmbH, Germany, 2003), p. 45.
[3] J. Ihleman, B. Wolf, P. Simon: Appl. Phys. A, **54,** (1992) 363.
[4] P. R. Herman, A. Oettl, K. P. Chen, R. S. Marjoribanks: Proc. SPIE, **3616,** (1999) 148.
[5] M. L. Ng, P. Herman, A. Nejadmalayeri, J. Li: Proc. SPIE, **5339,** (2004) 24-29.
[6] J. Wang, H. Niino, A. Yabe: Appl. Phys. A, **68,** (1999) 111.
[7] J. Wang, H. Niino, A. Yabe: Proc. SPIE, **3933**, (2000) 347.
[8] X. Ding, Y. Kawaguchi, H. Niino, A. Yabe: Proc. SPIE, **4830**, (2003) 156.
[9] J. Wang, H. Niino, A. Yabe: Appl. Surf. Sci., **154-155**, (2000) 571.
[10] C. Vass, B. Hopp, T. Smausz, F. Ignacs: Thin Solid Films, **453-454**, (2004) 121.
[11] C. Vass, T. Smausz B. Hopp: J. Phys. D: Appl. Phys., **37**, (2004) 2449.
[12] Y. Kawaguchi, X. Ding, A. Narazaki, T. Sato, H. Niino: Appl. Phys. A, **80**, (2005) 275.
[13] G. Kopitkovas, T. Lippert, C. David, S. Canulescu, A. Wokaun, J. Gobrecht: J. Photochem. Photobiol. A, **166**, (2004) 135.
[14] G. Kopitkovas, T. Lippert, C. David, R. Sulcas, J. Hobley, A. Wokaun, J. Gobrecht: Proc. SPIE, **5662**, (2004) 515.
[15] K. Zimmer, R. Böhme, A. Brau, B. Rauschenbach, F. Bigl: Appl. Phys. A, **74**, (2002) 453.
[16] G. Kopitkovas, T. Lippert, C. David, A. Wokaun, J. Gobrecht: Thin Solid Films, **453-454**, (2004) 31.
[17] R. Böhme, A. Braun, K. Zimmer: Appl. Surf. Sci., **186**, (2002), 276.
[18] R. Böhme, D. Spemann, K. Zimmer: Thin Solid Films, **453-454**, (2004) 127.

(Received: April 4, 2005, Accepted: August 29, 2005)